RESEARCH PAPER

Computational Profiling and Molecular Docking of Carissa Carandas Bioactives Against Alzheimer's Disease Targets

Karthigadevi Kamalakannan[1], Shanmuganathan Seetharaman[2], Anbazhagan Sockalingam[3], Kavimani Subramanian[4], K Reeta VijayaRani[5], Vijayan Venugopal[6]*

[1]Associate Professor, Department of Pharmacology, Surya School of Pharmacy, Surya Group of Institutions, Vikravandi, Villupuram – 605 652, Tamilnadu, India; Research Scholar, School of Pharmacy, SBV Pondicherry Campus, Sri Balaji Vidyapeeth (Deemed-to be-University), Puducherry-607402, India.
*[2]*Professor, Department of Pharmaceutics, School of Pharmacy, SBV Pondicherry Campus, Sri Balaji Vidyapeeth (Deemed-to be-University), Puducherry -607402, India.*
[3]Professor, Department of Pharmaceutical chemistry, Surya School of Pharmacy, Surya Group of Institutions, Vikravandi, Villupuram – 605 652, Tamilnadu, India.
[4]Professor, Department of Pharmacology, College of Pharmacy, Mother Theresa Post graduate and Research Institute of Health Sciences, Indira Nagar, Gorimedu, Puducherry-605 006, India.
[5]Professor, Department of Pharmaceutics, Surya School of Pharmacy, Surya Group of Institutions, Vikravandi, Villupuram – 605 652, Tamilnadu, India.
[6]Professor, Department of Pharmaceutics, School of Pharmacy, SBV Pondicherry Campus, Sri Balaji Vidyapeeth (Deemed-to be-University), Puducherry -607402, India.
[1]ekarthi1612@gmail.com, [2]shanmuganathan@sbvu.ac.in, [3]anbazhagans@gmail.com, [4]drkavimani@gmail.com, [5]reeta_rani07@yahoo.co.in, [6]vijayan@gmail.com
[1]ORCID ID: 0009-00003-6930-6075, [2]ORCID ID: 0000-0003-3735-1560, [3]ORCID ID: 0009-0002-3582-0191, [4]ORCID ID: 0000-0002-9630-1160 and [5]ORCID ID: 0000-0002-7040-6757
Corresponding author: Prof. Shanmuganathan Seetharaman, E-mail:shanmuganathan@sbvu.ac.in

Received: 24th April, 2026; Revised: 20th May 2026; Accepted: 30th June, 2026; Available Online: 10th July, 2026

ABSTRACT

Background: Despite decades of research, a disease-modifying cure for Alzheimer's disease (AD) has remained elusive, compelling investigators to seek novel pharmacological candidates. Key mechanistic targets under active exploration include acetylcholinesterase (AChE), the β-secretase enzyme BACE1, glycogen synthase kinase-3β (GSK-3β), and the TNF-α converting enzyme (TACE). This study leveraged GC-MS/MS-guided phytochemical identification alongside computational docking simulations to evaluate constituents of Carissa carandas fruit against these four molecular targets.

Objectives: This investigation set out to characterize previously unreported secondary metabolites from C. carandas fruit and evaluate their promise as anti-AD scaffolds through virtual screening.

Methods: Ethanolic extraction via Soxhlet apparatus was applied to powdered C. carandas fruit. Twelve volatile constituents were resolved by GC-MS/MS, five of which represent novel records for this species. AutoDock 4.2 was employed for molecular docking against BACE1 (PDB: 4K9H), TACE (PDB: 1ZXC), GSK-3β (PDB: 6GN1), and AChE (PDB: 4EY7), benchmarked against donepezil.

Results: Five phytoconstituents showed competitive free binding energies relative to the reference drug across all four targets. Swiss ADME-based in silico profiling indicated satisfactory oral bioavailability, intestinal permeability, and safety parameters.

Conclusions: The ethanolic fruit extract of C. carandas yielded five pharmacologically promising constituents—Alanyl-β alanine TMS derivative, l-Alanine N-ethoxycarbonyl-isohexyl ester, 3-O-Methyl-d-glucose, β D-Glucopyranoside methyl 3,6-anhydro-, and Oxalic acid cyclohexylmethyl isohexyl ester—that fulfilled rule of 5 criteria and demonstrated favorable ADMET characteristics. Although computational outcomes are encouraging, progression toward therapeutic application demands thorough in vivo validation, bioavailability testing, and dose-response characterization.

Keywords: *Alzheimer disease, acetylcholinesterase inhibition, β-amyloid aggregation, Carissa carandas, in silico docking*

**Author for Correspondence: shanmuganathan@sbvu.ac.in*

How to cite this article: Kamalakannan K, Seetharaman S, Sockalingam A, Subramanian K, VijayaRani KR and Venugopal V., Computational Profiling and Molecular Docking of Carissa Carandas Bioactives Against Alzheimer's Disease Targets. Int J Drug Deliv Technol. 2026;16(7): 728-743. DOI: 10.25258/ijddt.16.7.76
Source of support: Nil.
Conflict of interest: None

1. INTRODUCTION

Karonda (*Carissa carandas*.L), a spiny evergreen plant classified within the Apocynaceae family, is widespread across the Indian subcontinent and yields compact, berry-type fruits valued in culinary traditions throughout northern India. Its architecture is defined by dichotomous branching, abbreviated internodes equipped with axillary thorns, and a robust woody framework; established plants attain heights in the range of 3–5 m [1]. Across traditional healing systems, the roots, foliage, and ripening fruits of this species have served as remedies for a broad array of ailments—from febrile illness and dermatological complaints to oral mucosal lesions, anorexia, and gastrointestinal disturbances [2, 3].

Experimental pharmacological work has corroborated many of these ethnobotanical claims, with reported activities spanning antimicrobial, analgesic, anti-inflammatory, antipyretic, antioxidant, hepatoprotective, antidiabetic, antihyperlipidemic, and anticonvulsant effects [4–7]. The fruit is a particularly notable source of ascorbic acid. In Ayurvedic texts, unripe karonda fruits are prescribed as anthelmintics, digestive stimulants, and antipyretics, and are also referenced in the management of biliary ailments, gastric pathologies, and rheumatic or neurological disorders [8].

From a neuropathological perspective, published evidence indicates that Carissa species exert meaningful effects on central nervous system function. Specifically, fruit extracts from C. carandas have demonstrated neuroprotective capacity, anticonvulsant effects, and broader neuropharmacological activity in preclinical settings [9]. These properties motivated the present inquiry into the plant's phytochemical constituents as potential modulators of AD-related biochemical targets.

AD is an age-associated, irreversible neurodegenerative condition underpinned by the pathological accumulation of amyloid-β (Aβ) plaques and hyperphosphorylated tau neurofibrillary tangles, which collectively impair synaptic function, erode episodic memory, and accelerate neuronal loss [10, 11]. Pharmacotherapies currently on the market—principally AChE inhibitors and NMDA receptor antagonists—confer only symptomatic benefit and are associated with side effects such as hepatic enzyme elevation, gastrointestinal intolerance, and appetite suppression, limiting patient adherence. Curcumin, an extensively studied natural compound, has shown capacity to antagonize Aβ deposition in vitro and in animal models, yet suboptimal transport across the blood–brain barrier (BBB) under physiological conditions curtails its translational utility [12, 13].

This therapeutic gap has intensified interest in natural product chemistry as a reservoir of structurally diverse bioactive scaffolds. Botanical sources have historically provided foundational leads for pharmaceutical development; the WHO estimates that plant-based traditional medicine remains the predominant primary healthcare resource for a substantial portion of the global population [14]. As a case in point, phytochemicals recovered from Opuntia ficus-indica cladodes were demonstrated to afford neuroprotection in an aluminum chloride-induced neurotoxicity rodent model [15]. Accordingly, the present study undertook comprehensive GC-MS/MS profiling of C. carandas ethanolic fruit extract and subjected the identified constituents to structure-based virtual screening against Aβ and AChE targets, aiming to identify improved lead candidates relative to current AD therapies.

2. MATERIALS AND METHODS

2.1. Reagents and Instrumentation

Chemical reagents and HPLC-grade solvents obtained from TCI Pvt. Ltd and Sigma-Aldrich (India) were employed at analytical-grade purity without additional purification steps. All chromatographic analyses were conducted on a Shimadzu GCMS-TQ8040 NX platform (Toshvin Analytical Pvt. Ltd., Mumbai) equipped with triple quadrupole MS/MS capability.

2.2. Procurement and Authentication of Plant Material

Mature fruits of C. carandas were field-collected in September 2023 from Amrithi Hills, Vellore District, Tamil Nadu, India. Taxonomic verification was performed by Dr. Sivasankar of Auroville Botanical Services, Puducherry, and a voucher specimen bearing accession number 13524 was lodged at the Auroville herbarium facility. Following collection, fruits were cleaned, de-seeded, sliced into thin sections, and desiccated under ambient conditions (25–30°C) over a 14-day period. The resulting dried material was then pulverized into fine powder and held under dark conditions at 20°C pending further processing.

2.3. Extraction Procedure

Powdered plant material (100 g) underwent hot continuous extraction in 500 mL absolute ethanol within a Soxhlet apparatus over a 48-hour extraction cycle, which was repeated with fresh solvent until the efflux became visually clear. The pooled extract was taken to dryness under reduced pressure via rotary evaporation and the resulting solid residue was sealed and refrigerated at 4°C until required [16].

2.4. Operational Parameters for GC-MS/MS Analysis

Chromatographic resolution was achieved on a Shimadzu GCMS-TQ8040 NX fitted with an AOC-20s autosampler and AOC-20i autoinjector, using a bonded-phase SH Rxi 5MS Sil fused-silica capillary column (30 m × 0.25 mm i.d.; 0.25 µm film). A stepwise temperature gradient was applied: initial hold at 80°C (2 min), ramp at 5°C/min to 150°C (5 min hold), and a final ramp to 280°C (8 min hold). Ultra-high purity helium served as carrier gas at 1.72 mL/min. A 6.0 µL aliquot was introduced under splitless/20:1 split conditions; the injection port and ion source were maintained at 230°C and 280°C, respectively. Electron ionization at 70 eV scanned the m/z window 45–350 over a 55-minute total run; solvent delay was set to 3.2 minutes. Each sample was pre-diluted in GC-grade methanol (Sigma-Aldrich) to achieve optical clarity before loading 2 mL of the upper phase into a pre-cleaned GC vial. Spectral identification relied on comparison of empirical fragmentation patterns with entries in the NIST08s, NIST08, and NIST14 reference libraries [17].

2.5. Molecular Docking Analysis

2.5.1. Preparation of Target Proteins

Four therapeutically validated AD-associated targets were chosen for this study. Crystal structures were downloaded from the RCSB Protein Data Bank [18]:

a) Human β-site APP cleaving enzyme 1, BACE1 (PDB: 4K9H)

b) Human glycogen synthase kinase-3 beta, GSK-3β (PDB: 6GN1)

c) Human TNF-α converting enzyme, TACE (PDB: 1ZXC)

d) Human acetylcholinesterase, AChE (PDB: 4EY7)

Standardized preparation of each structure involved removal of bound water molecules and co-crystallized heteroatoms that could interfere with active site accessibility, while catalytically relevant metal ions were retained. All docking runs utilized the ligand-free (apo) protein conformations.

2.5.2. Ligand Structure Preparation

PubChem-sourced 2D chemical structures corresponding to the GC-MS-identified phytocompounds (**Table 1 & supplementary Figure S1**) were converted to energy-minimized 3D conformations using the GAFF molecular mechanics force field as implemented in the Avogadro modeling suite.

2.5.3. Docking Workflow

All docking experiments were executed within the AutoDock 4.2 framework, treating each ligand–receptor combination independently. Kollman united-atom charges and polar hydrogen atoms were appended to receptor structures; rotatable bonds in the ligand were assigned from the literature-reported binding pocket geometry. A cubic grid enclosing 50 × 50 × 50 points at 0.375 Å resolution was centered on the orthosteric binding cavity (within 5 Å radius). One hundred Lamarckian genetic algorithm (LGA) runs were performed per docking experiment under default convergence settings. Resultant conformational clusters were ranked according to predicted free binding energy (ΔG), and the lowest-energy pose within the most populated cluster—together with its hydrogen-bonding contacts—was selected for downstream analysis [19].

2.6. ADME/Tox - In Silico Assessment

Canonical SMILES strings for each lead compound were retrieved from PubChem (https://pubchem.ncbi.nlm.nih.gov) and submitted to the SwissADME server (http://www.swissadme.ch) for evaluation of absorption, distribution, metabolism, and excretion parameters. Assessments encompassed Lipinski Ro5 compliance, predicted human intestinal absorption, BBB penetration potential, cytochrome P450 isoform inhibition, and bioavailability scoring [19, 20].

3. RESULTS

3.1. GC-MS/MS Phytoconstituent Profiling

Chromatographic separation of the C. carandas ethanolic fruit extract generated twelve well-resolved peaks spanning a retention time window of 3.52 to 20.51 minutes (Fig. 1). The identity of each peak, verified against NIST mass spectral libraries, is presented in Table 1 below.

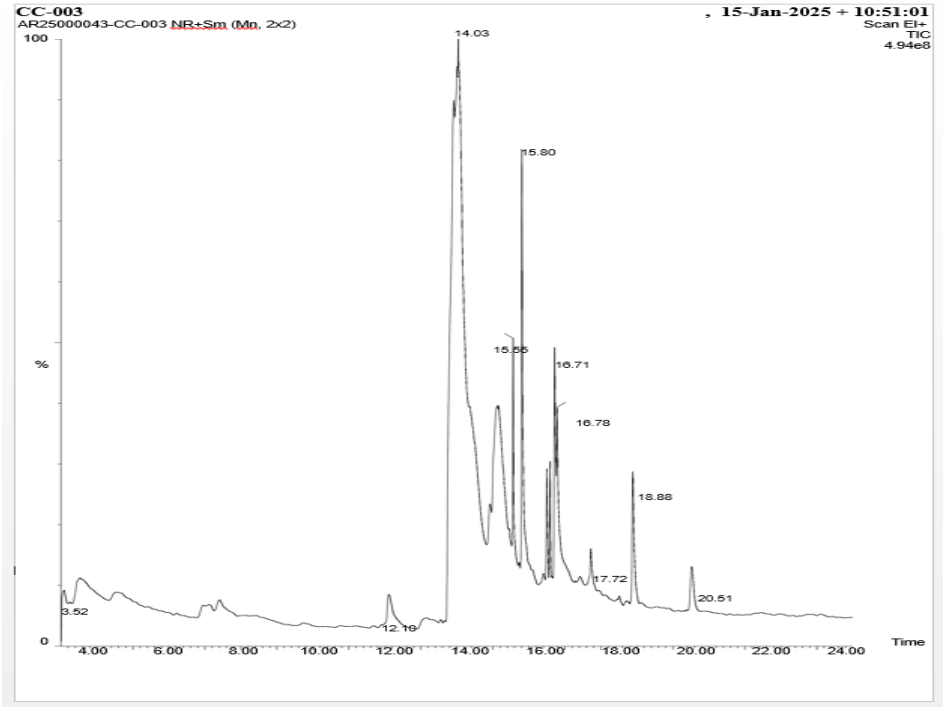

Fig 1: Gas Chromatogram of C.carandas Fruit Ethanolic Extract

Table 1. Chromatographic retention times and compound identities from GC-MS/MS analysis of C. carandas ethanolic fruit extract.

No.	Retention Time (min)	Compound Identity
1	3.52	Silane, [(1,1-dimethyl-2-propenyl)oxy]dimethyl
2	12.10	Alanyl-β alanine, TMS derivative
3	14.03	l-Alanine, N-ethoxycarbonyl-, isohexyl ester
4	15.10	3-O-Methyl-d-glucose
5	15.55	β D-Glucopyranoside, methyl 3,6-anhydro-
6	15.80	1,2-Hydrazinedicarboxamide
7	16.62	9,9-Dimethoxybicyclo[3.3.1]nona-2,4-dione
8	16.71	Oleic Acid
9	16.78	Dodecanoic acid, 2-penten-1-yl ester
10	17.72	Oxalic acid, cyclohexylmethyl isohexyl ester
11	18.82	6-Undecyl-5,6-dihydro-2H-pyran-2-one
12	20.51	Carbonic acid, neopentyl cyclohexylmethyl ester

Supplementary figures S1: Ligand structures/Preparation corresponding to the GC-MS-identified phytocompounds

Fig S1.1

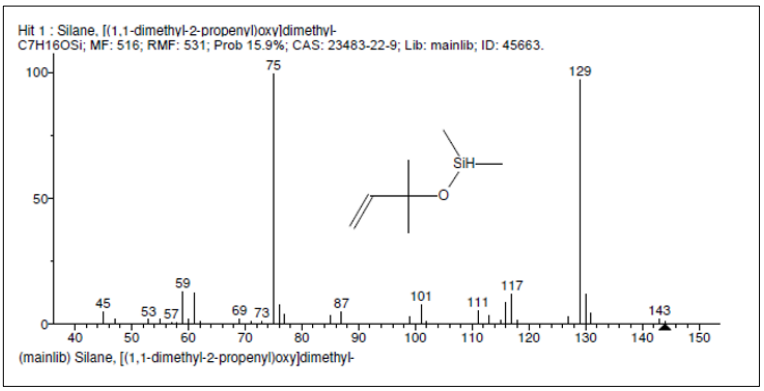

Fig S1.2

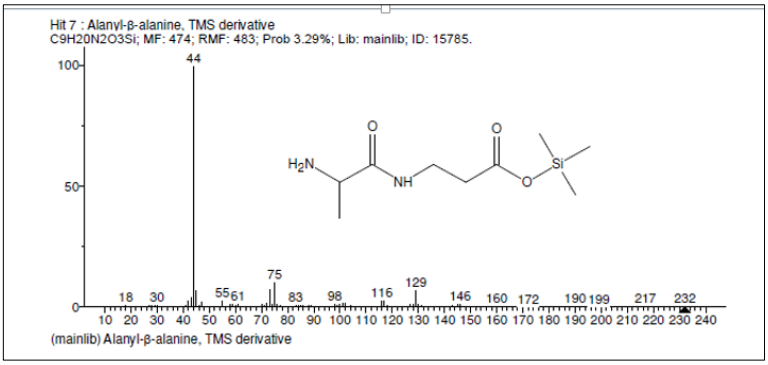

Fig S1.3

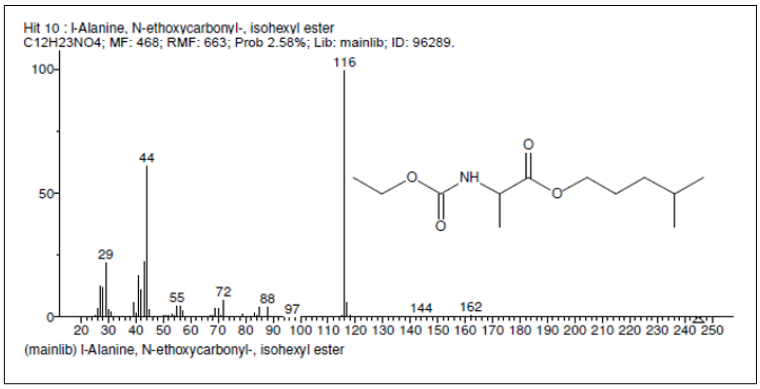

Fig S1.4

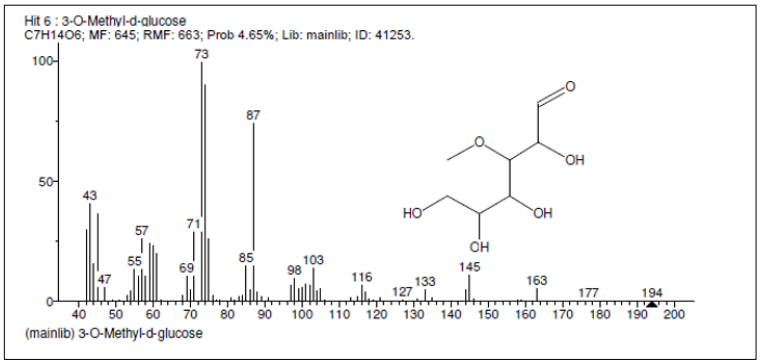

Fig S1.5

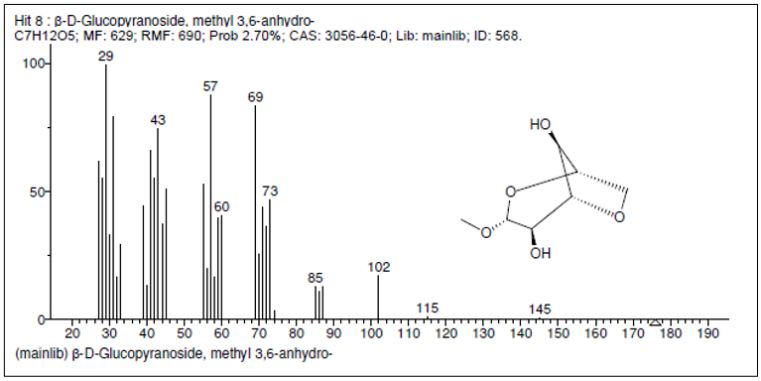

Fig S1.6

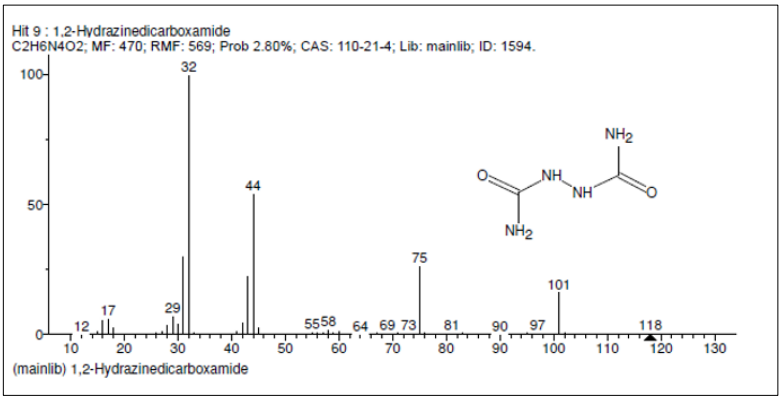

Fig S1.7

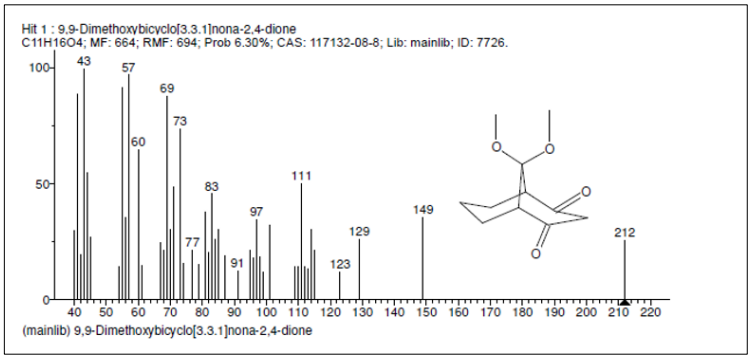

Fig S1.8

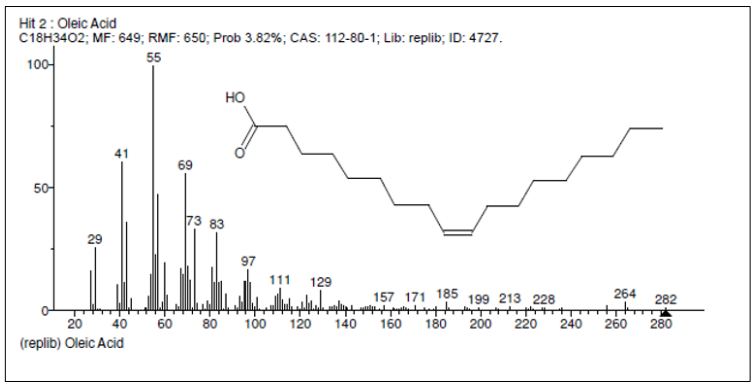

Fig S1.9

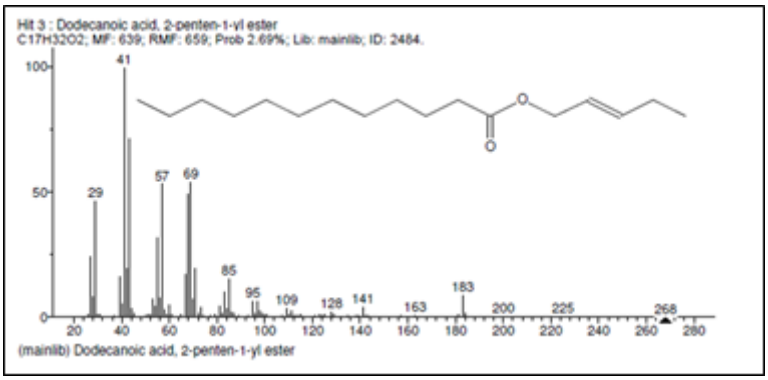

Fig S1.10

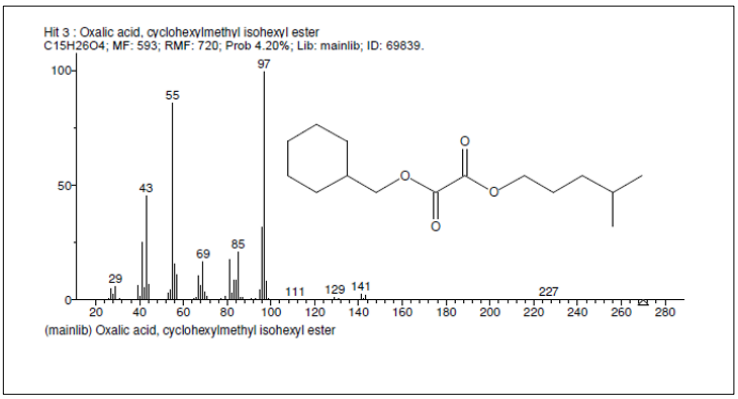

Fig S1.11

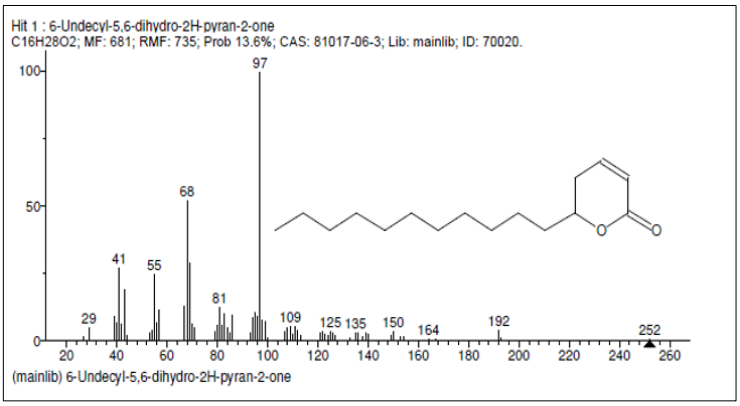

Fig S1.12

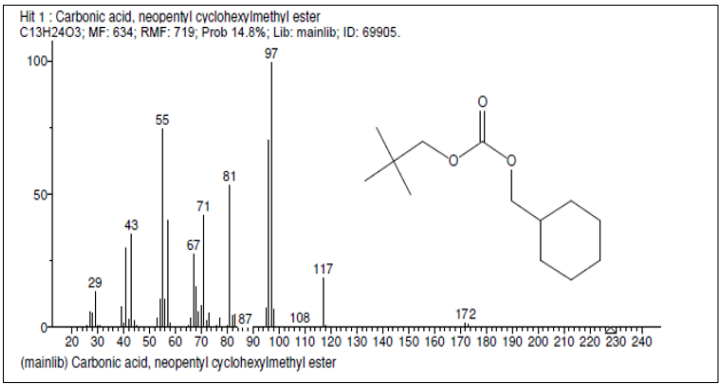

3.2. Computational Docking Outcomes

Supplementary Table 1: Predicted free binding energies (ΔG, kcal/mol) for screened phytocompounds docked against four AD-relevant proteins, with donepezil as comparator.

Compound No.	Target Protein	PDB ID	ΔG (kcal/mol)
2	BACE1	4K9H	-6.98
3	BACE1	4K9H	-5.10
4	BACE1	4K9H	-3.30
5	BACE1	4K9H	-4.49
10	BACE1	4K9H	-6.20
Donepezil	BACE1	4K9H	-7.47
2	GSK-3β	6GN1	-4.56
3	GSK-3β	6GN1	-5.10
4	GSK-3β	6GN1	-2.19
5	GSK-3β	6GN1	-3.96
10	GSK-3β	6GN1	-6.10
Donepezil	GSK-3β	6GN1	-8.85
2	TACE	1ZXC	-6.74
3	TACE	1ZXC	-5.95
4	TACE	1ZXC	-3.21
5	TACE	1ZXC	-5.21
10	TACE	1ZXC	-6.98
Donepezil	TACE	1ZXC	-7.50
2	AChE	4EY7	-6.55
3	AChE	4EY7	-6.08
4	AChE	4EY7	-2.96
5	AChE	4EY7	-5.19
10	AChE	4EY7	-7.58
Donepezil	AChE	4EY7	-7.08

AD Target proteins -BACE1: Human β-site APP cleaving enzyme 1, (PDB: 4K9H): GSK-3β: Human glycogen synthase kinase-3 beta, (PDB: 6GN1); TACE: Human TNF-α converting enzyme, (PDB: 1ZXC); AChE: Human acetylcholinesterase, (PDB: 4EY7); Donepezil –Standard.

Supplementary Figure S2: 3D Interaction between Selected 5 Compounds with 4 AD Receptors

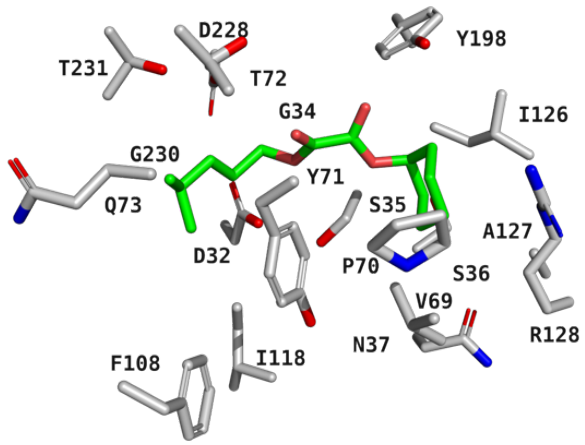

Figure S2. 1: 3D interaction between Human BACE1 (PDB ID:4K9H) with ligand (10); Oxalic acid, cyclohexylmethyl isohexyl ester

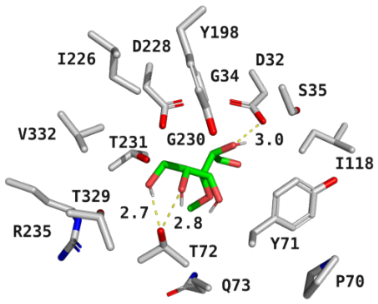

Figure S2. 2: 3D interaction between Human BACE1 (PDB ID:4K9H) with ligand 3-O-Methyl-d-glucose

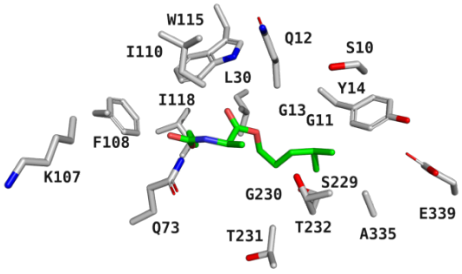

Figure S2.3: 3D interaction between Human BACE1 (PDB ID:4K9H) with ligand l-Alanine, N-ethoxycarbonyl-, isohexyl ester

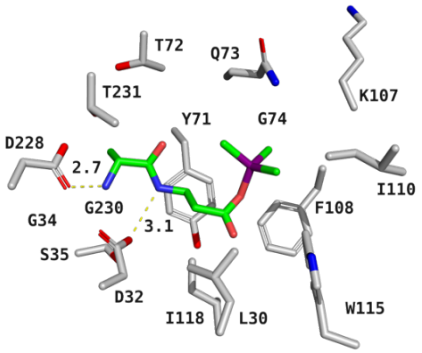

Figure S2.4: 3D interaction between Human BACE1 (PDB ID:4K9H) with ligand Alanyl- β alanine, TMS derivative

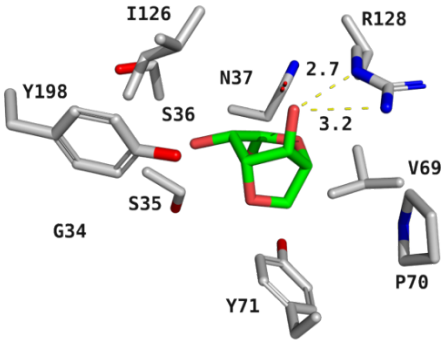

Figure S2.5: 3D interaction between Human BACE1 (PDB ID:4K9H) with ligand β D-Glucopyranoside, methyl 3,6-anhydro-

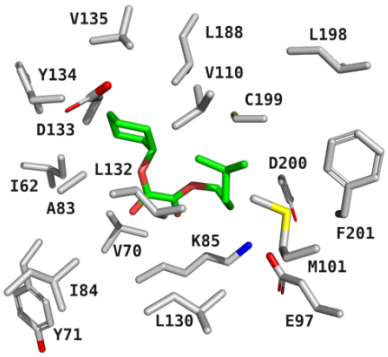

Figure S2.6: 3D interaction between Human Glycogen synthase kinase-3 beta (PDB ID:6GN1) with ligand (10); Oxalic acid, cyclohexylmethyl isohexyl ester

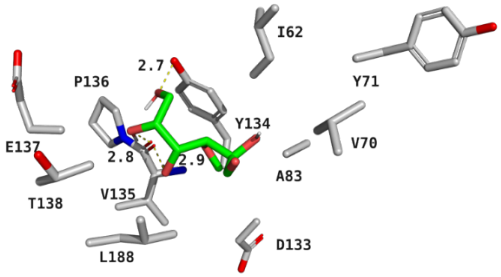

Figure S2.7: 3D interaction between Human Glycogen synthase kinase-3 beta (PDB ID:6GN1) with ligand 3-O-Methyl-d-glucose

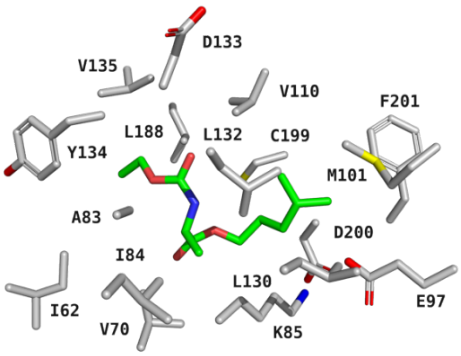

Figure S2.8: 3D interaction between Human Glycogen synthase kinase-3 beta (PDB ID:6GN1) with ligand l-Alanine, N-ethoxycarbonyl-, isohexyl ester

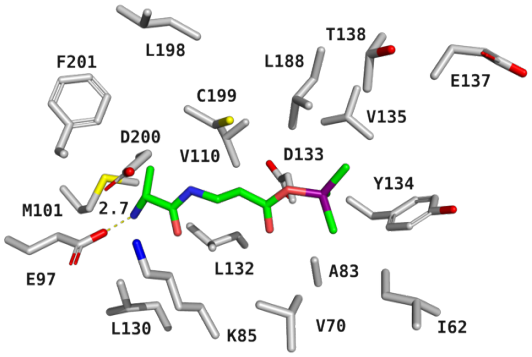

Figure S2.9: 3D interaction between Human Glycogen synthase kinase-3 beta (PDB ID:6GN1) with ligand Alanyl- β alanine, TMS derivative

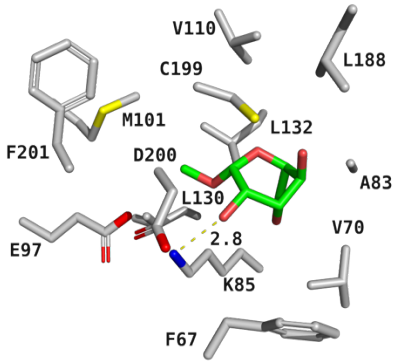

Figure S2.10: 3D interaction between Human Glycogen synthase kinase-3 beta (PDB ID:6GN1) with ligand β D-Glucopyranoside, methyl 3,6-anhydro

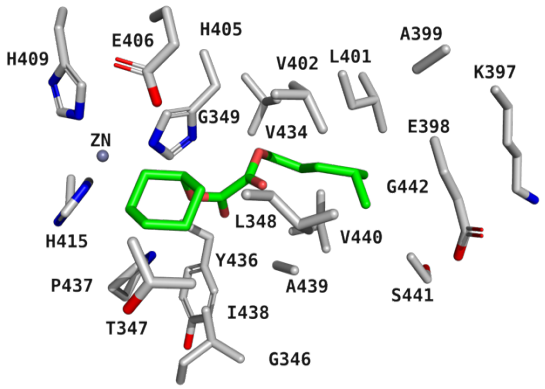

Figure S2.11: 3D interaction between Human TNF-alpha converting enzyme (PDB ID:1ZXC)with ligand (10); Oxalic acid, cyclohexylmethyl isohexyl ester

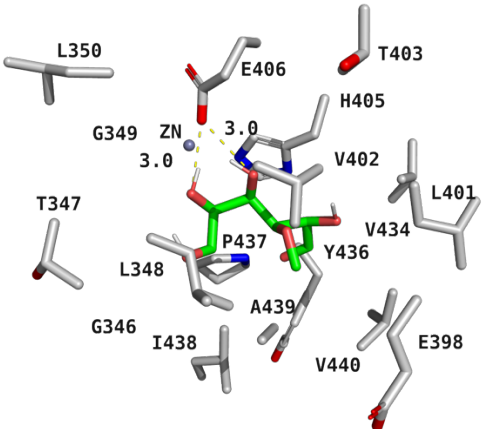

Figure S2.12: 3D interaction between Human TNF-alpha converting enzyme (PDB ID:1ZXC) with ligand 3-O-Methyl-d-glucose

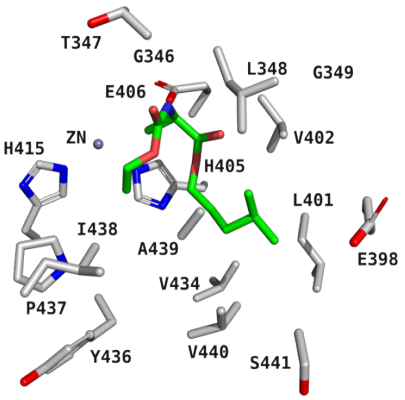

Figure S2.13: 3D interaction between Human TNF-alpha converting enzyme (PDB ID:1ZXC)with ligand l-Alanine, N-ethoxycarbonyl-, isohexyl ester

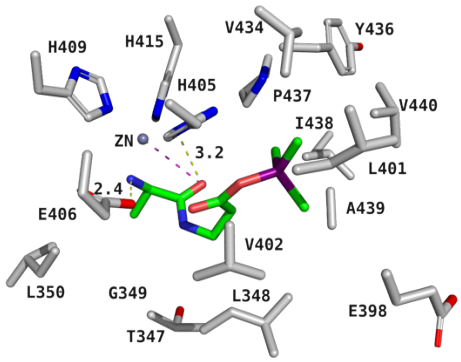

Figure S2.14: 3D interaction between Human TNF-alpha converting enzyme (PDB ID:1ZXC)with ligand Alanyl- β alanine, TMS derivative

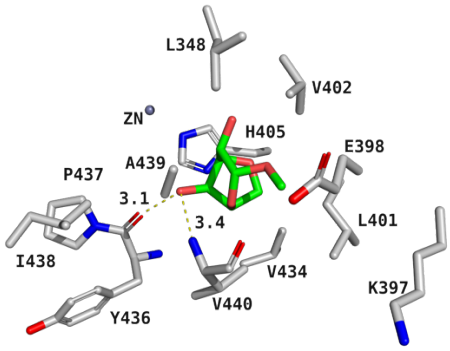

Figure S2.15: 3D interaction between Human TNF-alpha converting enzyme (PDB ID:1ZXC) with ligand β D-Glucopyranoside, methyl 3,6-anhydro

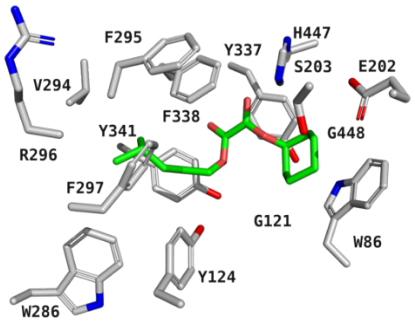

Figure 16: 3D interaction between Human Acetylcholinesterase (PDB ID:4EY7)with ligand (10); Oxalic acid, cyclohexylmethyl isohexyl ester

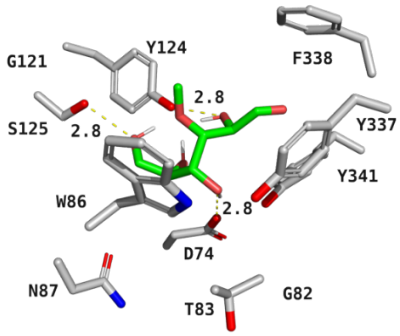

Figure S2.17: 3D interaction between Human Acetylcholinesterase (PDB ID:4EY7) with ligand 3-O-Methyl-d-glucose

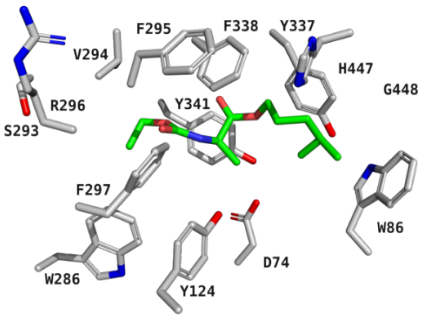

Figure S2.18: 3D interaction between Human Acetylcholinesterase (PDB ID:4EY7) with ligand l-Alanine, N-ethoxycarbonyl-, isohexyl ester

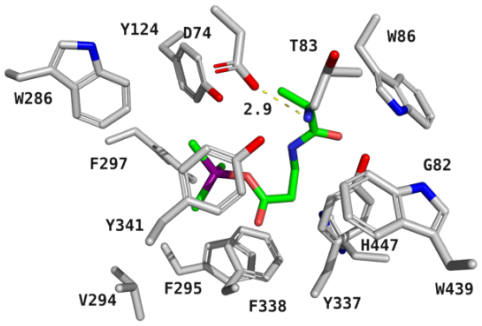

Figure S2.19: 3D interaction between Human Acetylcholinesterase (PDB ID:4EY7) with ligand Alanyl-β alanine, TMS derivative

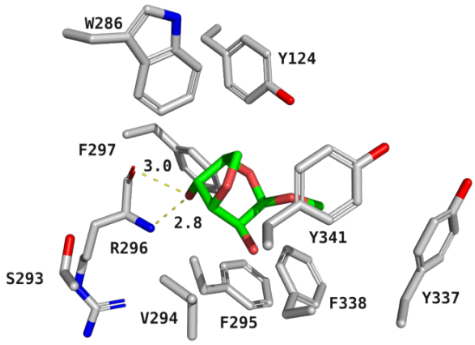

Figure S2.20: 3D interaction between Human Acetylcholinesterase (PDB ID:4EY7) with ligand β D-Glucopyranoside, methyl 3,6-anhydro

3.2.1. Overall Binding Energy Profile

Predicted 3D ligand geometries used for docking are depicted in **Supplementary Fig. S1**. A consolidated binding energy matrix for all tested phytocompound–target combinations is provided in **Supplementary Table 1**. Hierarchical clustering of molecular interaction fingerprints across target proteins is shown in **Supplementary Fig. S2**.

3.2.2. BACE1 Interactions (PDB: 4K9H)

Binding affinities of the five candidate phytoconstituents toward BACE1 varied substantially. The dipeptide derivative Alanyl-β alanine TMS (compound 2) recorded the highest affinity at −6.98 kcal/mol, and Oxalic acid cyclohexylmethyl isohexyl ester (compound 10) followed at −6.20 kcal/mol. Intermediate scores were observed for l-Alanine N-ethoxycarbonyl-isohexyl ester (−5.10 kcal/mol) and β D-Glucopyranoside methyl 3,6-anhydro- (−4.49 kcal/mol), while 3-O-Methyl-d-glucose displayed the weakest interaction at −3.30 kcal/mol. The standard drug donepezil scored −7.47 kcal/mol.

3.2.3. GSK-3β Interactions (PDB: 6GN1)

Against the kinase target GSK-3β, compound 10 again led the phytocompound panel with −6.10 kcal/mol, outperforming all remaining test compounds. l-Alanine N-ethoxycarbonyl-isohexyl ester and Alanyl-β alanine TMS recorded −5.10 and −4.56 kcal/mol, respectively. Compounds 5 and 4 showed weaker engagement at −3.96 and −2.19 kcal/mol. Donepezil achieved the overall highest affinity at −8.85 kcal/mol for this target.

3.2.4. TACE Interactions (PDB: 1ZXC)

Compound 10 performed exceptionally against TACE, reaching −6.98 kcal/mol—numerically equivalent to the donepezil reference value (−7.50 kcal/mol). Compound 2 scored −6.74 kcal/mol, while compound 3 (l-Alanine N-ethoxycarbonyl-isohexyl ester) registered −5.95 kcal/mol. Compounds 5 and 4 trailed with −5.21 and −3.21 kcal/mol, respectively.

3.2.5. AChE Interactions (PDB: 4EY7)

Notably, compound 10 surpassed donepezil at the AChE active site, attaining a binding energy of −7.58 kcal/mol versus −7.08 kcal/mol for the reference compound. Compound 2 scored −6.55 kcal/mol and compound 3 reached −6.08 kcal/mol. Compounds 5 and 4 contributed −5.19 and −2.96 kcal/mol, respectively.

3.3. ADMET Computational Profiling

SwissADME-based pharmacokinetic evaluation of the five candidate molecules is summarized in Table 2, encompassing key absorption, metabolic stability, and toxicological indices.

Table 2. Physicochemical and predicted ADME/Tox properties of five phytocompounds identified in C. carandas fruit extract.

Property	Oxalic acid, cyclohexylmethyl isohexyl ester	3-O-Methyl-d-glucose	l-Alanine, N-ethoxycarbonyl-, isohexyl ester	Alanyl-β alanine, TMS derivative	β D-Glucopyranoside, methyl 3,6-anhydro-
Formula	C15H26O4	C7H14O6	C12H24NO4	C9H20N2O3Si	C7H12O5
Mol. Weight	270.34	194.18	246.32	232.35	176.17
H-bond donors	0	4	2	2	2
H-bond acceptors	4	6	4	4	5

Property	Oxalic acid, cyclohexylmethyl isohexyl ester	3-O-Methyl-d-glucose	l-Alanine, N-ethoxycarbonyl-, isohexyl ester	Alanyl-β alanine, TMS derivative	β D-Glucopyranoside, methyl 3,6-anhydro-
Rotatable bonds	8	6	9	7	1
Intestinal absorption	High	Low	High	High	High
BBB Permeation	Yes	No	Yes	No	No
Bioavailability score	0.55	0.55	0.56	0.55	0.55
CYP1A2 inhibitor	Yes	No	No	No	No
CYP2C19 inhibitor	Yes	No	No	No	No
CYP2C9 inhibitor	No	No	No	No	No
CYP2D6 inhibitor	No	No	No	No	No
CYP3A4 inhibitor	No	No	No	No	No
TPSA	52.6	107.22	75.63	81.42	68.15
log Kp (cm/s)	-4.84	-9.54	-6.24	-7.52	-8.52
Lipinski compliant	Yes	Yes	Yes	Yes	Yes
Drug likeness	Good	Good	Good	Good	Good
Carcinogenicity	No	No	No	No	No
Acute toxicity	2.23	2.37	1.32	1.36	2.35

4. DISCUSSION

The ethnobotanical and neuropharmacological profile of C. carandas makes it a rational subject for AD-directed phytochemical investigation. Soxhlet extraction of desiccated fruit powder with ethanol generated a chemically diverse extract, from which GC-MS/MS resolved ten previously undocumented phytoconstituents in this species, each assigned based on retention time and NIST spectral library matches.

From a neuropathological standpoint, AD unfolds through a multistep cascade involving aberrant Aβ peptide fibrillogenesis—a central precipitating event. Under physiological conditions, Aβ monomers circulate in soluble form within cerebrospinal fluid; in diseased tissue, however, they nucleate into oligomers and elongated fibrils that exert cytotoxicity through mechanisms that are not yet fully understood. Since Aβ fibrillation is linked to downstream tau pathology, synaptic dysfunction, and neuronal apoptosis, pharmacological interference with this aggregation cascade carries both preventive and therapeutic significance [21]. Concurrently, cholinergic deficiency—a hallmark of AD progression—has made AChE a primary therapeutic target, as inhibiting this enzyme sustains synaptic acetylcholine and partially compensates for degenerating cholinergic neurons. Although donepezil, rivastigmine, galantamine, and tacrine have obtained regulatory approval as AChE inhibitors for AD, their impact is strictly palliative and is associated with adverse events that limit prolonged administration.

Reviewing the docking data systematically, compound 10 (Oxalic acid cyclohexylmethyl isohexyl ester) delivered the most consistently potent binding across all four AD targets, with ΔG values ranging from −6.10 to −7.58 kcal/mol. Notably, its predicted AChE affinity (−7.58 kcal/mol) exceeded that of the clinical reference drug donepezil (−7.08 kcal/mol), while its TACE affinity (−6.98 kcal/mol) closely approximated donepezil's reference value. In the AutoDock scoring framework, increasingly negative ΔG values denote tighter ligand–receptor

complementarity, meaning these differences carry mechanistic relevance. Compound 4 (3-O-Methyl-d-glucose) recorded the weakest predicted binding (−2.19 to −3.30 kcal/mol), suggesting limited structural complementarity with these target cavities. Compounds 2, 3, and 5 occupied intermediate affinity positions.

The clinical significance of AChE inhibition in AD therapy rests on the cholinergic hypothesis, which attributes much of the cognitive decline in AD to progressive loss of basal forebrain cholinergic neurons and consequently reduced synaptic ACh availability [22]. Compound 10's superiority over donepezil at this target, while computationally derived, warrants validation through enzymatic inhibition assays.

Neuroinflammatory mechanisms—particularly those mediated through the TNF-α signaling axis—have been implicated in AD pathogenesis, with TACE playing a central regulatory role by cleaving membrane-bound TNF-α precursor into its soluble, pro-inflammatory form. Elevated soluble TNF-α concentrations have been documented in AD brain tissue relative to age-matched controls [23], making TACE a strategically valuable neuroinflammatory target. The docking profiles of the screened phytocompounds against TACE align with trends observed in prior virtual screening campaigns targeting alternative natural molecules [23].

BACE1 represents the rate-limiting enzymatic step in Aβ production; cleavage of amyloid precursor protein (APP) at the β-site initiates the amyloidogenic cascade, rendering BACE1 inhibition one of the most pursued strategies in AD drug discovery [24]. A major structural impediment is BACE1's unusually voluminous active site, which creates steric challenges for small-molecule inhibitor design [25]. GSK-3β is also therapeutically relevant, as its hyperactivation in AD tissue contributes to abnormal tau phosphorylation at multiple serine/threonine residues, accelerating tangle formation and neurodegeneration [26, 27]. Compounds 2 and 10 displayed noteworthy binding toward both BACE1 and GSK-3β, suggesting multi-target potential.

When assessed for drug-likeness, all five shortlisted molecules satisfied Lipinski's Rule of Five thresholds, a widely accepted filter for predicting oral bioavailability. None of the compounds showed predicted carcinogenicity. Regarding CNS penetrance—a decisive criterion for any anti-AD candidate—compounds 10 and 3 demonstrated positive BBB permeation scores, whereas the remaining three did not. Intestinal absorption was predicted as high for four of five compounds, with 3-O-Methyl-d-glucose being the exception due to its higher topological polar surface area. Acute oral toxicity estimates were within non-hazardous ranges for all candidates. Compound 10 additionally demonstrated CYP1A2 and CYP2C19 inhibitory potential, which may need consideration during further preclinical safety profiling.

Collectively, these in silico findings position several secondary metabolites of C. carandas as viable starting points for anti-AD drug design. However, the inherent limitations of computational approaches—including the absence of protein dynamics, solvent effects, and intracellular context—underscore that these predictions must be followed up with rigorous in vitro enzymatic assays, cell-viability studies, and ultimately, in vivo pharmacokinetic and efficacy testing.

5. CONCLUSION

Through integrated GC-MS/MS metabolite profiling and structure-based virtual screening, this study has established that the ethanolic fruit extract of C. carandas harbors pharmacologically relevant phytochemicals with multi-target inhibitory potential against key AD-associated proteins. Among twelve resolved constituents, five compounds—Alanyl-β alanine TMS derivative, l-Alanine N-ethoxycarbonyl-isohexyl ester, 3-O-Methyl-d-glucose, β D-Glucopyranoside methyl 3,6-anhydro-, and Oxalic acid cyclohexylmethyl isohexyl ester—demonstrated satisfactory predicted binding affinities against BACE1, GSK-3β, TACE, and AChE.

Virtual screening platforms such as molecular docking serve as powerful, resource-efficient tools for narrowing large chemical spaces to high-priority leads, reducing downstream experimental attrition. Integrating pharmacokinetic pre-filtering through Lipinski's criteria further enriches the candidate pool with compounds more likely to survive clinical development phases. In this study, all five lead molecules cleared the Ro5 threshold, none exhibited predicted mutagenicity or carcinogenicity, and most showed high intestinal absorption. Compound 10 was particularly distinguished—outperforming donepezil at the AChE site and approximating its affinity at TACE, while also passing BBB permeation screening.

These outcomes nominate C. carandas fruit as a scientifically valuable source of potential anti-AD scaffolds and justify advancement of the identified compounds, particularly compound 10 into in vitro enzyme inhibition studies, followed by in vivo pharmacological characterization and structural optimization campaigns. Further synthetic derivatization may yield analogues with enhanced selectivity, CNS penetrance, and reduced metabolic liability compared to the parent phytochemicals.

ACKNOWLEDGEMENT

The authors would like to thank IIT, Hyderabad & GreenMed Labs Research Services, Chennai, Tamilnadu, India for providing facilities and services required to complete the study. All authors are thankful to their respective Departments/Universities for successful completion of this study.

AUTHOR CONTRIBUTIONS

Writing- original draft: K.K., and S.S.; Supervision: K.K., S.S., and S.A.; Resources: S.K., K.R., and V.V; Writing-review and editing: K.K., S.S., S.A., S.K.., K.R., and V.V; All authors have read and agreed to the published version of the manuscript.

CONFLICT OF INTEREST
The authors declare that there is no conflict of interest.

FUNDING
There is no funding availed for this work

ETHICAL APPROVAL
Not applicable

ABBREVATION

AChE	:	Acetylcholinesterase
AD	:	Alzheimer's disease
ADME/Tox	:	**Absorption, Distribution, Metabolism, Excretion, and Toxicity**
Aβ	:	Amyloid-β
BACE1	:	β-site APP cleaving enzyme 1
BBB	:	Blood Brain Barrier
g	:	Gram
GC-MS/MS	:	Gas chromatography-Mass spectrometry
GSK-3β	:	Glycogen synthase kinase-3 beta
kcal/mol	:	**kilocalories per mole**
ml	:	Milli litre
NMDA	:	N-methyl D-aspartate receptor antagonists
TACE	:	TNF-α converting enzyme

REFERENCES

1. Jayakumar K, Muthuraman B. Nutritional profile and ethnobotanical uses of the karonda fruit (Carissa carandas Linn.). World Sci News. 2018; 96: 217–224. https://doi.org/10.3390/antiox13091037.
2. Madhuri S, Neelagund SE. Assessment of antioxidant, antidiabetic, and DNA-protective properties of Carissa carandas fruit preparations. Int J Adv Res Dev. 2019; 4: 75–82. https://doi.org/10.3390/antiox13091038.
3. Vysakh A, Ratheesh M, Rajmohanan TP, et al. Polyphenolic constituents from virgin coconut oil attenuate adjuvant-induced arthritis in rats via antioxidant and anti-inflammatory pathways. Int Immunopharmacol. 2014; 20: 124–130. DOI: 10.1016/j.intimp.2014.02.026. PMID: 24613207.
4. David M, Karekalamnavar G. Spectroscopic characterization and in vitro antimicrobial and anticancer evaluation of Carissa carandas L. aqueous ethanolic fruit extract. J Adv Sci Res. 2015; 6: 10–13.
5. Itankar PR, Lokhande SJ, Verma PR, et al. Antidiabetic activity of unripe Carissa carandas Linn. fruit extract. J Ethnopharmacol. 2011; 135: 430–433. DOI: 10.1016/j.jep.2011.03.036. PMID: **21439367.**
6. Siddiqi, R. Naz, S. Ahmad, S. Sayeed, S.A. Antimicrobial activity of the polyphenolic fractions derived from *Grewia asiatica*, *Eugenia jambolana* and *Carissa carandas*. *Int. J. Food Sci. Technol.* 2011; *46*: 250–256. https://doi.org/10.1111/j.1365-2621.2010.02480.x.
7. Prakash R. Itankar, Sarika J. Lokhande, Prashant R. Verma , Sumit K. Arora, Rajesh A. Sahu , Arun T. Patil . Antidiabetic potential of unripe *Carissa carandas* Linn. fruit extract. Journal of Ethnopharmacology. 2011; 135(2): 430-433.
8. Morton JF. Fruits of warm climates-Creative Resource Systems. Inc. Winterville, N.C, USA. 1987; 503.
9. Srinivasa Rao Kareti , Subash P. In Silico Molecular Docking Analysis of Potential Anti-Alzheimer's Compounds Present in Chloroform Extract of Carissa carandas Leaf Using Gas Chromatography MS/MS. Current Therapeutic Research. 2020; 93: 100615. https://doi.org/10.1016/j.curtheres.2020.100615.
10. Ahmed, S. Khan ,S.T. Zargaham, M.K. Khan, A.U. Khan, S. Hussain, A. Uddin, J.Khan, A. Al-Harrasi, A. Potential therapeutic natural products against Alzheimer's disease with Reference of Acetylcholinesterase. Biomed. Pharmacother. 2021; 139: 111609. doi: 10.1016/j.biopha.2021.111609. PMID: 33915501.
11. Kanathip Singsai, Natthanicha Ladpala, Natthan Dangja, Thanyaret Boonchuen, Niracha Jaikhamfu, and Pirinyapat Fakthong . Effect of Streblus asper Leaf Extract on Scopolamine-Induced Memory Deficits in Zebrafish: The Model of Alzheimer's Disease. Advances in Pharmacological and Pharmaceutical Sciences. 2021: 7 pages. pages https://doi.org/10.1155/2021/6666726. PMID: 33987539.
12. Swetha, G.; Anjali Raj, Saniya Tabassum. Oxidative stress in alzheimer's disease–evaluating the amyloid beta hypothesis. Int J Curr Pharm Res. 2021; 13(5): 32-38. DOI:10.22159/ijcpr.2021v13i5.1906.
13. Paresh Doshi, Jaslok Hospital and Research Centre. Efficacy and Safety of Curcumin Formulation in Alzheimer's Disease. NCT01001637.2023.
14. Worku Chekol Tassew, Yeshiwas Ayal Ferede ,Agerie Mengistie Zeleke, Getaw Wubie Assefa, Prevalence and associated factors of herbal medicine use among patients living with chronic disease in Ethiopia: A systematic review and meta-analysis. Metabolism. 2024; 21: 10028. DOI: 10.1016/j.metop.2024.100280.
15. Seham S. El-Hawarya, Mansour Sobehb,f, Wafaa K. Badrc, Mohamed A.O. Abdelfattahd, Zeinab Y. Alie, Mona E. El-Tantawyc, Mohamed A. Rabeha, Michael Winkb . HPLC-PDA-MS/MS profiling of

secondary metabolites from Opuntia f icus-indica cladode, peel and fruit pulp extracts and their antioxidant, neuroprotective effect in rats with aluminum chloride induced neurotoxicity. Saudi Journal of Biological Sciences. 2020; 27: 2829–2838. **DOI:** 10.1016/j.sjbs.2020.07.003

16. Mishra, CK.; Pattnaik, AK.; Dagur, P.; Kumar, D.; Ghosh M. Excision and incision wound healing activity of apigenin (4',5,7-trihydroxyflavone) containing extracts of Carissa carandas Linn. fruits. Phcog Mag. 2022; 18: 502-509. DOI:10.4103/pm.pm-100-21.
17. Hasan MR, Haque MM, Hoque MdA, Sultana S, Rahman MM, Ali Shaikh MdA, et al. Antioxidant activity study and GC-MS profiling of Camellia sinensis Linn. Heliyon. 2024; 10(1): e23514. doi:10.1016/j.heliyon.2023.e23514
18. Gnanaraj C, Sekar M, Fuloria S, et al. Computational molecular docking analysis of karanjin against Alzheimer and Parkinson disease targets. Molecules. 2022; 27: 2834. https://doi.org/ 10.3390/molecules27092834. https://doi.org/10.3390 /molecules27092834.
19. Israa J. Hakeem, Molecular docking analysis of acetylcholinesterase inhibitors for Alzheimer's disease management . Bioinformation. 2023; 19(5): 565-570. DOI: 10.6026/97320630019565
20. Subash P., Srinivasa Rao Kareti In silico molecular docking analysis for potential anti-Alzheimer's compounds from the methanolic leaf extract of Erythroxylum monogynum using Gas chromatography–mass spectrometry. Journal of Saudi Chemical Society. 2021; 25: 101285. https://doi.org/10.1016/j.jscs.2021.101285
21. Worku Chekol Tassew, Yeshiwas Ayal Ferede ,Agerie Mengistie Zeleke, Getaw Wubie Assefa, Prevalence and associated factors of herbal medicine use among patients living with chronic disease in Ethiopia: A systematic review and meta-analysis Metabolism Open. 2024; 21: 10028. DOI: 10.1016/j.metop.2024.100280.
22. Rees TM, Brimijoin S. Cholinergic mechanisms and the role of acetylcholinesterase in the neuropathology of Alzheimer disease. Drugs Today. 2003; 39: 75–83. DOI: 10.1358/dot.2003.39.1.722650.
23. Cheng X, Yang L, He P, Li R, Shen Y. Selective activation of tumor necrosis factor receptors in Alzheimer disease versus non-demented aging. J Alzheimer Dis. 2010; 19: 621–630. **10.3233/JAD-2010-1253**.
24. Vassar R. Clinical prospects for BACE1 inhibitor therapeutics in Alzheimer disease. Alzheimer Res Ther. 2014; 6: 89. DOI: 10.1186/s13195-014-0089-7.
25. Koelsch G. Structural and catalytic properties of BACE1 and their implications for inhibitor-based AD therapy. Molecules. 2017; 22: 1723. https://doi.org/10.3390/molecules22101723.
26. Eldar-Finkelman H, Martinez A. Progress and challenges in targeting GSK-3 for CNS disorders. Front Mol Neurosci. 2011; 4: 32. DOI:10.3389/fnmol.2011.00032.
27. Bhat R, Xue Y, Berg S, et al. Crystallographic and biological characterization of the GSK-3-selective inhibitor AR-A014418. J Biol Chem. 2003; 278: 45937–45945. DOI: 0.1074/jbc.M308332200.